Meteorol. Appl. 3, 147–155 (1996)

Exploring the effects of different types of model initialisation: simulation of a severe air-pollution episode in Athens, Greece

K Lagouvardos, V Kotroni and G Kallos, *University of Athens, Department of Applied Physics, Meteorology Laboratory, Ippokratous 33, 10680, Athens, Greece*

A combined modelling system consisting of a meteorological model (Colorado State University/ Regional Atmospheric Modelling System) and a transport package (Hybrid Particle and Concentration Transport Model) is used. The simulations were performed using two types of model initialisation: the first with ECMWF gridded analysis data and the second with one sounding profile. The modelling system has been used to simulate an important air-pollution episode in the Athens urban area. This area is characterised by complex and variable topographic features, and the associated local atmospheric circulations play a significant role in defining the transport and dispersion conditions over the area. The advantages and shortcomings of both types of initialisation, and more specifically the capability of the model to represent and reproduce the local-scale conditions and the dispersion of air pollutants, are discussed.

1. Introduction

The spatial and temporal resolution of meteorological data assimilated in a numerical model is very important when performing fine-grid simulations over areas characterised by a complex boundary layer. In this study, the effects of model initialisation are explored through the combined use of the meteorological model CSU/RAMS (Colorado State University/Regional Atmospheric Modelling System) and the dispersion model HYPACT (Hybrid Particle and Concentration Transport Model). The use of this modelling system permits:

(a) The exploration of the advantages and shortcomings of two types of model initialisation: the uniform initialisation using one sounding profile and the variable initialisation with gridded analysis data provided over a larger area.
(b) The demonstration of the capability of this modelling system to simulate successfully air pollution episodes over an urban area (Athens), characterised by significant terrain complexity.

The Greater Athens Area (GAA) has been selected for the simulations because it has been plagued by air-quality problems during the last decade, due to the significant population shift and increased industrialisation and use of motorised vehicles. Moreover, the GAA is characterised by significant terrain variability and complexity. The complexity of the terrain leads to the formation of local atmospheric circulations, which determine the transport and dispersion conditions over the area.

2. Description of the combined modelling system RAMS-HYPACT

2.1. The RAMS model

The Regional Atmospheric Modelling System (RAMS) is a highly versatile system developed at Colorado State University and ASTER Division of Mission Research Corporation for simulating and forecasting meteorological phenomena, and for displaying the results (Walko & Tremback, 1991; Pielke *et al.*, 1992). Its major components are:

(a) An isentropic analysis package which uses observed meteorological data to prepare initial data for the atmospheric model.
(b) An atmospheric model which performs the actual simulations.
(c) A post-processing visualisation and analysis package which interfaces atmospheric model output with a variety of visualisation software utilities.

The atmospheric model uses the full set of primitive dynamical equations which govern atmospheric motions, and supplements these equations with optional parameterisation schemes for turbulent diffusion, solar and terrestrial radiation, moist processes (including the formation and interaction of clouds and precipitation liquid, and ice hydrometeors), sensible and latent heat exchanges (between the atmosphere, multiple soil layers and a vegetation canopy), the kinematic effects of terrain, and cumulus convection.

RAMS uses a two-way interactive grid nesting which allows local fine-mesh grids to resolve small-scale

atmospheric systems, while simultaneously modelling the large-scale environment of the systems on a coarser grid. The most important features of RAMS are summarised in Pielke *et al.* (1992). Specific applications of this modelling system to air-quality studies are reviewed in Pielke *et al.* (1991), and Lyons *et al.* (1993). Recent air-quality studies based on the application of RAMS can be found in Fast *et al.* (1995), Poulos & Bossert (1995), and Lyons *et al.* (1995).

2.2. The HYPACT model

The Hybrid Particle and Concentration Transport Package (HYPACT) was developed at the Colorado State University and ASTER Division of Mission Research Corporation (Tremback *et al.*, 1994). It is a combination of a Lagrangian particle model and an Eulerian concentration transport model. HYPACT uses a level 2.5 turbulent closure scheme based on the prognostic turbulent kinetic energy calculated by RAMS. With the Lagrangian part of the model, the particles are advected with mean and random turbulent wind components using the velocity and turbulence fields simulated by RAMS. When the pollutant is adequately resolved on the grid, the particles are converted to a concentration field and handled in a Eulerian manner. The source configurations of HYPACT are very flexible: any number of sources can be specified anywhere in the domain and configured as a point, line, area, or volume source, while these sources can be instantaneous, intermittent or continuous. A recent application of the combined RAMS and HYPACT model can be found in Lyons *et al.* (1994).

3. The air pollution episode of 18 January 1993

The Greater Athens Area (GAA) is characterised by significant terrain variability. The GAA includes the cities of Athens and Piraeus, and their suburbs. This area is located in a Basin surrounded by mountains on three sides and open to the sea (with the Saronic Gulf) on the fourth side (Figure 1). The three main mountains are Hymettus (1050 m) to the east, Pendeli (1100 m) to the north–northeast, and Parnitha (1400 m) to the north–northwest. To the west of the basin is the mountain Aegaleo, 450 m high. There are hills up to 200 m inside the basin (Pnyka, Lycabettus, and Tourcovounia). The main axis of the basin is south–southwest to north–northeast (25 km) and its area is approximately 450 km^2. The industrial area is concentrated at the south–southwest edge of the basin. Other important sources of air pollution are the Piraeus harbour located to the west–southwest, and Hellinicon airport at the south–southeast edge of the basin.

Under a weak synoptic flow, mesoscale thermal circulations develop over the GAA. These local-scale circulations are induced by the complex terrain and, according to the synoptic classification scheme presented in Kallos *et al.* (1993) and Kassomenos *et al.* (1995), they influence the transport and dispersion of air pollutants over the GAA, forming, in general, bad dispersion conditions in the Attica Peninsula and Saronic Gulf.

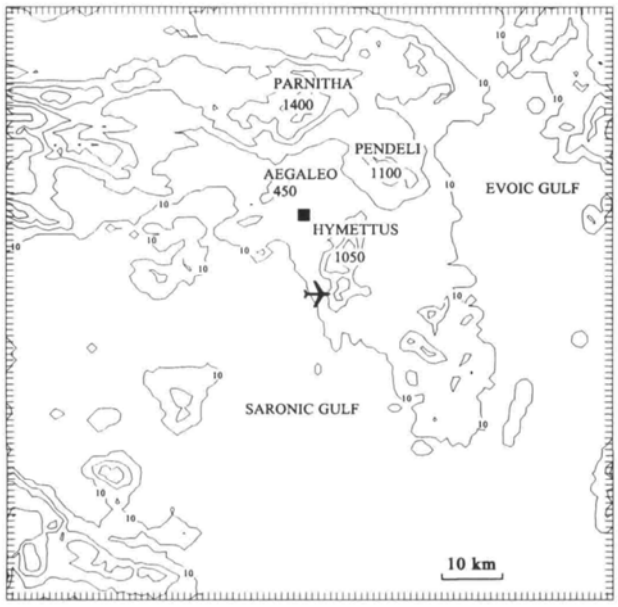

Figure 1. Map of the Greater Athens Area. Elevation is contoured every 250 m. The black rectangle denotes the location of the air-quality monitoring station located in the centre of Athens (37.98° N, 23.73° E). The location of the upper-air station (Athens Airport) is also shown.

For the present simulations a winter case has been selected. More specifically, during the period from 17 to 18 January, 1993, the Mediterranean region was characterised by stationary conditions. As it can be seen in the surface analysis at 0000 UTC on 18 January, 1993 (Figure 2), a high pressure system dominated the greatest part of the Mediterranean region, southern Europe and northern Africa, giving rise to light winds. Warm air masses had been transported over the Mediterranean region. This synoptic situation was characteristic of a blocking high. Inspection of three soundings at 0000 UTC, for 16 to 18 January, 1993 (Figure

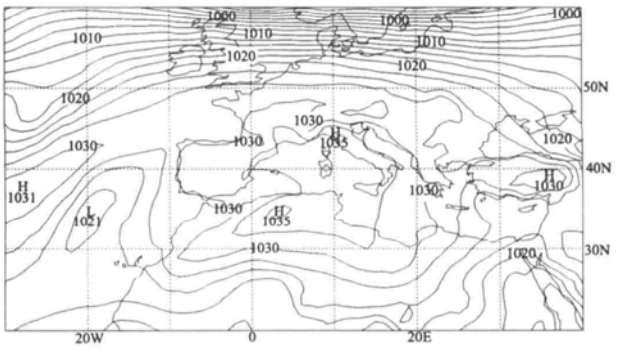

Figure 2. Surface analysis for 0000 UTC, 18 January, 1993 (with 2.5 hPa interval).

3), shows a warming of about 5 °C in the layer 1000 to 800 hPa from 0000 UTC, 16 January to 0000 UTC, 17 January, while in the same layer a warming of about 2 °C is evident from 0000 UTC 17 January to 0000 UTC 18 January. The sounding from 18 January shows an important surface inversion of about 6.5 °C within the first 1 km. Light winds prevail up to the 400 hPa level.

The synoptic situation reported above results in bad dispersion conditions in the GAA. Indeed, on 18 January, 1993, a very important air-pollution episode was reported in the area of Athens. During air-pollution episodes, that is when air pollution reaches emergency action levels, restrictions are imposed, mainly in the use of civilian cars in GAA and on the operation of industry. The concentration of NO_2 recorded by an urban monitoring station in the centre of Athens reached a maximum of 554 $\mu g\ m^{-3}$ during this day. This concentration was the highest reported in 1993, and it was above the emergency action level (500 $\mu g\ m^{-3}$), while the early warning limit value is 200 $\mu g\ m^{-3}$.

4. Setup of the modelling system

The effects of model initialisation will be investigated through the application of the combined modelling system (RAMS and HYPACT) in simulating the air-pollution episode on 18 January, 1993.

Two nested grids were selected for the meteorological simulations. The outer grid had a mesh of 50×40 points and 10 km horizontal grid increment, while the inner grid had a mesh of 62×62 points and 2 km horizontal grid increment, centred over the GAA (37.85° N, 23.65° E). Twenty-one levels following the topography were used in both grids, having a 120 m vertical spacing near the ground, stretching to 1 km at an altitude of 6.5 km and remaining constant up to about 12.5 km. Topography files with 5′ resolution for the outer grid and 30 sec. resolution for the inner grid, as well as sea-surface temperature climatological files with 1 degree resolution were used. Test runs have been performed in order to choose the appropriate resolution of the inner grid which can describe the local characteristics of the GAA. The grids were selected in such a way so as to avoid the lateral boundary problems identified by Kallos & Kassomenos (1994) which might result in a failure in representing the recirculation of air pollutants and/or the ventilation in the GAA.

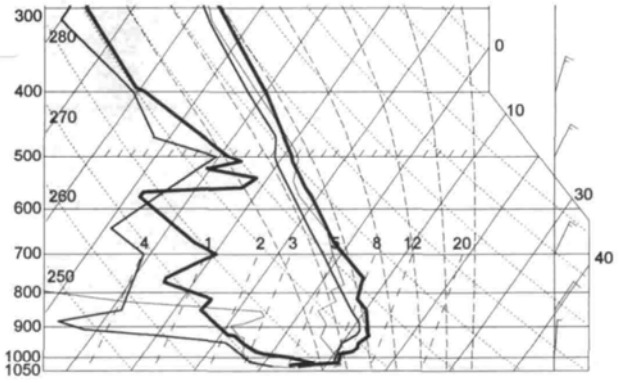

Figure 3. Standard skew T-log *p* diagram depicting the temperature, dewpoint and wind profile at Athens station (16716) for 0000 UTC 16 January, 1993 (light lines), 0000 UTC, 17 January (solid lines) and 0000 UTC, 18 January (bold lines). One full barb equals 5 ms^{-1} and one half barb equals 2.5 ms^{-1}.

RAMS model can be initialised in two ways.

(a) Using a sounding profile ('horizontally homogeneous' or 'uniform' initialisation).
(b) Using gridded ECMWF analysis files ('variable' initialisation).

Both types of initialisation are used in the present study in order to explore the effect of each one of them on the simulation of an air-pollution episode. Under the prevailing synoptic conditions (weak pressure gradient over the area of interest allowing the development of local circulations), which remain unchanged during at least 24 hours, the uniform initialisation with the sounding of 0000 UTC, 18 January, 1993 (depicted in Figure 3) can be considered as appropriate. For the variable initialisation, 1° gridded analysis files from ECMWF were used. The ECMWF data are objectively analysed on isentropic surfaces from which they are interpolated to the RAMS grid. These fields were used in order to nudge the lateral boundary region of the coarser grid every six hours. The simulation has been performed for a period of 40 hours, starting at 0000 UTC, 18 January 1993.

The dispersion model (HYPACT) is driven by the RAMS meteorological output data. These data include the wind, potential temperature, eddy diffusion coefficients and turbulent kinetic energy at all model levels and grid points. For the purpose of this study, the Eulerian option of HYPACT has been used. For that reason, an emission inventory set has been used for nine different sources of pollutants. This set contained the 24-hour evolution of NO_x emissions for an area of 50 km around the city centre and it included emissions from mobile sources (private cars, duty tracks, buses and two wheelers) as well as from stationary sources (heating and industry). It should be noted that the emission inventories are mean values for the whole year and therefore they cannot represent the emission specific characteristics for each day (circulation, industrial activities, etc.). The run of the dispersion model started at 0000 UTC, 18 January, 1993, in order to investigate the build-up effects of the model during the first hours of the simulations.

5. Results from the modelling system

5.1. Model comparisons

The wind fields predicted from both runs will be now discussed and compared. Hereafter these runs will be denoted by:

UI – uniform initialisation.
VI – variable initialisation.

Figure 4 shows the wind flow near the surface in the inner grid, predicted from the UI run. At 0600 UTC (Figure 4(*a*)), the wind flow is from an easterly direction over the Saronic Gulf, while over the Evoic Gulf there are northerlies. Light winds prevail over almost the whole domain, except over the mountains. At 0900 UTC (Figure 4(*b*)), thermal circulations begin to develop in the layer 0–200 m above the ground. These thermal circulations are intensified during the day, reaching a speed of about 5 m $^{-1}$ (Figure 4(*c*)) and last until 1500 UTC. At this time the northerly winds over the Saronic Gulf penetrate inland. Inspection of the wind field at higher levels (not shown) revealed that the thermal circulations extend up to about 350 m while above this level winds are turning to the north-northeast following the synoptic-scale forcing. At 1900 UTC (Figure 4(*d*)), a weak variable flow is evid-

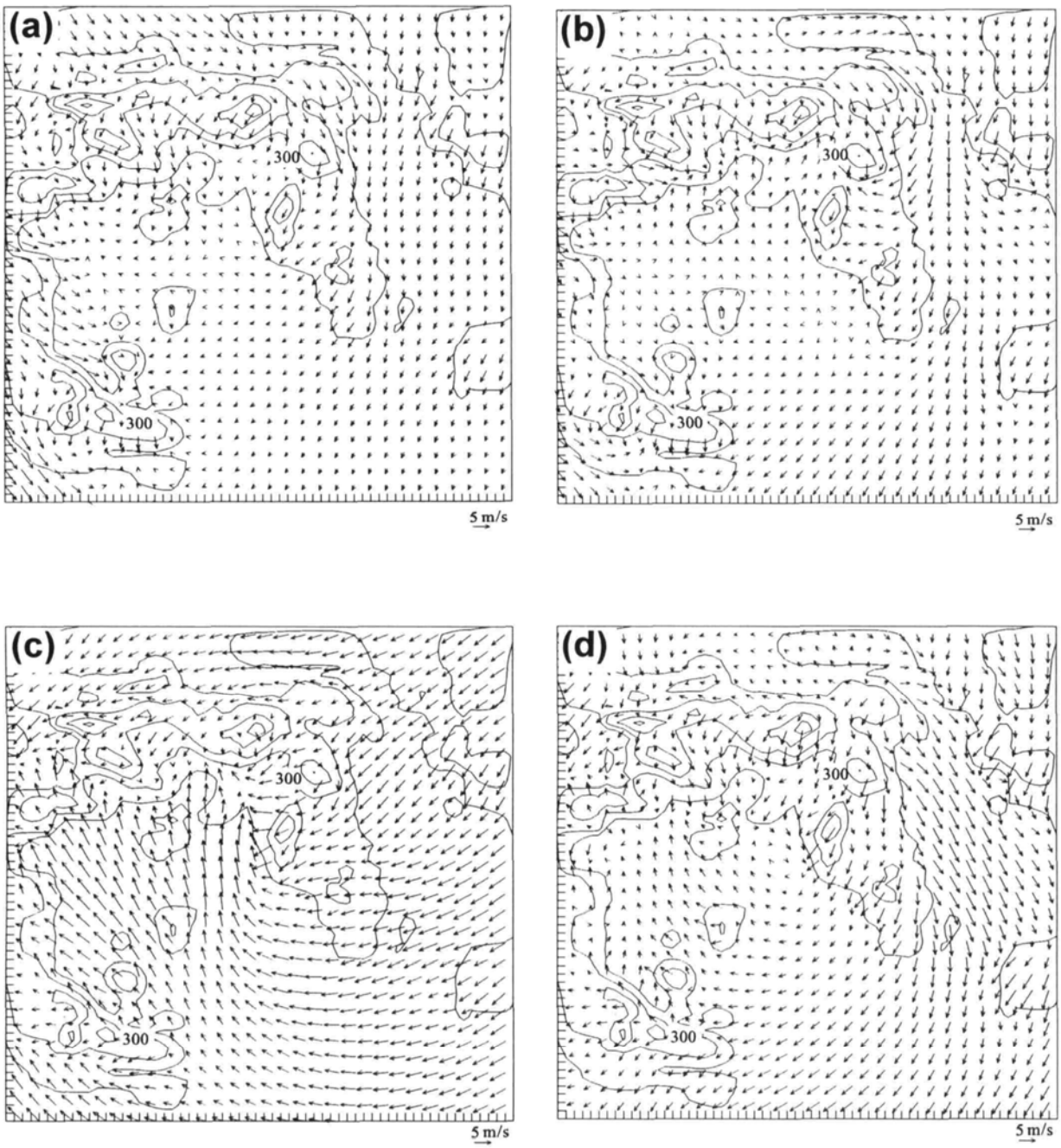

Figure 4. Wind field at $z = 50$ m on the inner grid, for the UI run , at (*a*) 0600 UTC, (*b*) 0900 UTC, (*c*) 1500 UTC and (*d*) 1900 UTC, on 18 January, 1993. Start time 0000 UTC, 18 January, 1993. The topography is contoured every 250 m.

ent over the Saronic Gulf, while over the Evoic Gulf the wind flow is stronger (7 m s^{-1}) from a north-westerly direction.

Figure 5 presents the wind flow near the surface in the inner grid, predicted from the VI run. The wind flow at 0600 UTC (Figure 5(*a*)) is very weak except over the mountains (as was also predicted by the UI run), while at 0900 UTC the beginning of the thermal circulations is also evident (Figure 5(*b*)). At 1500 UTC (Figure 5(*c*)) these thermal circulations reach their maximum intensity with a southerly flow of 5 m s^{-1} over the Saronic Gulf which penetrates inland. A difference between the VI and the UI run is that in the VI run the flow over the Evoic Gulf is from the southeast, while in the UI run the flow is from the northeast. At 1900 UTC (Figure 5(*d*)) the flow patterns predicted by both runs are very similar except in the southern part of the domain where the flow in the VI run is weaker than the UI run and from a westerly direction. In general the wind fields predicted by the two runs are in very good agreement and this is due to the very stable prevailing conditions.

The surface concentration fields calculated from HYPACT (where the RAMS UI run predicted fields are assimilated) are given in Figure 6. At 0600 UTC,

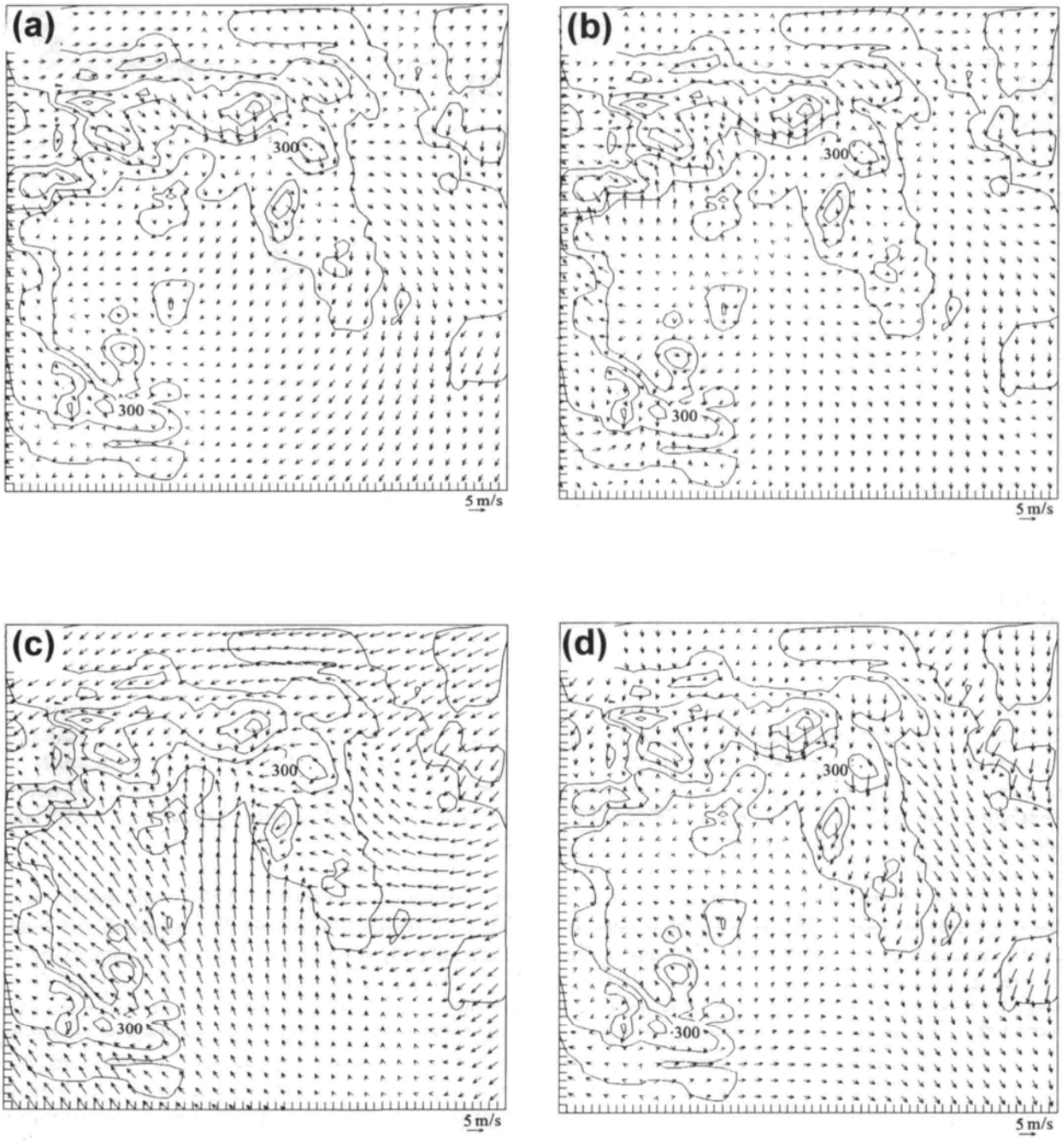

Figure 5. Wind field at $z = 50$ m on the inner grid, for the VI run , at (*a*) 0600 UTC, (*b*) 0900 UTC, (*c*) 1500 UTC and (*d*) 1900 UTC, on 18 January, 1993. Start time 0000 UTC, 18 January, 1993. The topography is contoured every 250 m.

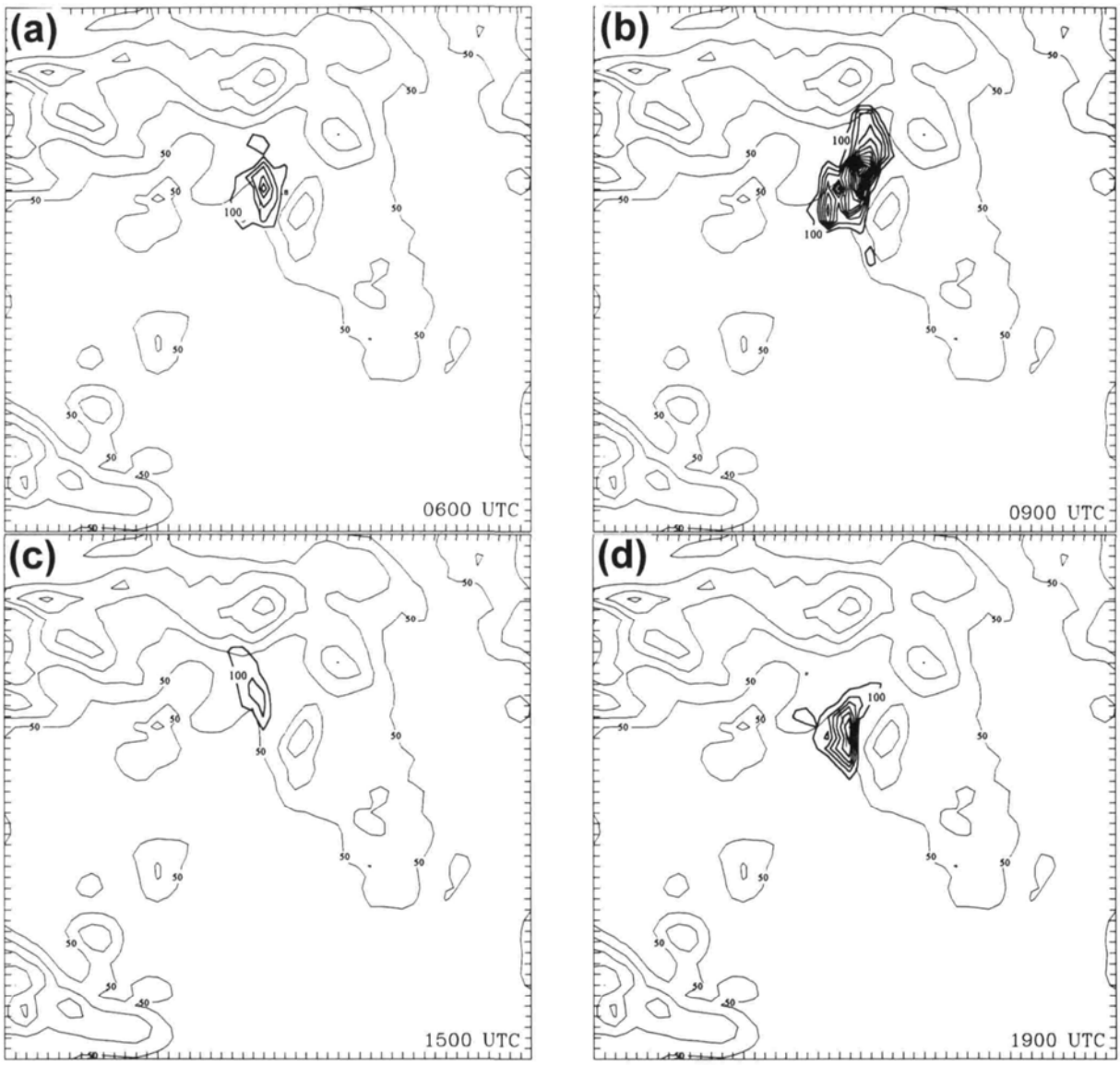

Figure 6. Horizontal cross-section of NO_x surface concentration in the inner grid (UI run), at (*a*) 0600 UTC, (*b*) 0900 UTC, (*c*) 1500 UTC and (*d*) 1900 UTC, 18 January, 1993. Isopleths of concentrations are every 100 μg m^{-3} (bold lines). Elevation is contoured every 250 m (light lines).

18 January, 1993 (Figure 6(*a*)), the pollutants begin to concentrate in the centre of Athens, where the largest part of the pollutants is emitted, and the largest concentration at this time is 579 µg m^{-3}. The maximum concentration of the day occurs at 0900 UTC, exceeding 1450 µg m^{-3}. This maximum concentration results from the trapping of pollutants due to the morning surface inversion, depicted in the sounding profile (Figure 3). As seen in Figure 6(*b*), the maximum is slightly advected to the north of the city, due to the development of thermal circulations at this time (very light sea-breeze and upslope flows – see Figure 4(*b*)). At 1500 UTC (Figure 6(*c*)) the pollutant concentrations are low, with a maximum of 238 µg m^{-3}. The second daily maximum occurs at 1900 UTC with a value of 706 µg m^{-3} (Figure 6(*d*)), but this is near the coast of the Saronic Gulf, due to the advection of the pollutants by the northerly flow (Figure 4(*d*)). Inspection of the individual contribution of each one of the pollutant sources (not shown) revealed that emission by private cars has the greatest contribution to the total surface concentrations, followed by emissions from industrial activity, heavy-duty trucks and buses.

The surface concentration fields calculated from HYPACT (where the RAMS VI run predicted fields are assimilated) are given in Figure 7. Comparison of the VI predicted concentration fields (Figure 7(*b*)) with the UI fields (Figure 6(*b*)) reveals that in the case of the VI run the model fails to reproduce the morning concentration maximum (it predicted a maximum concentration of about 618 µg m^{-3} compared to 1450 µg m^{-3} of the UI run). The daily maximum concentration of about 1030 µg m^{-3} was predicted at 1900 UTC (Figure 7(*d*)).

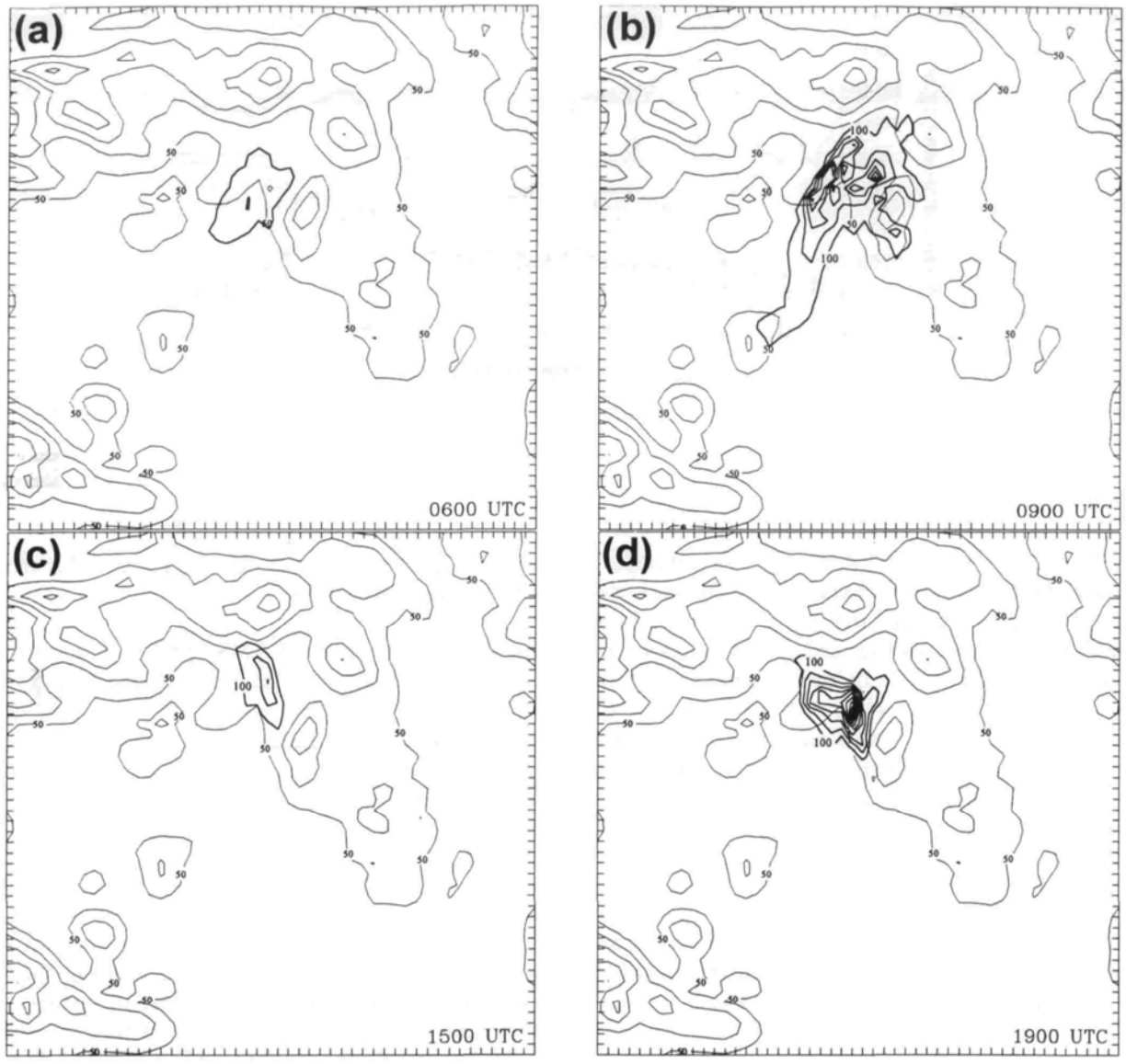

Figure 7. Horizontal cross-section of NO_x surface concentration in the inner grid (VI run), at (*a*) 0600 UTC, (*b*) 0900 UTC, (*c*) 1500 UTC and (*d*) 1900 UTC, 18 January, 1993. Isopleths of concentrations are every 100 $\mu g\ m^{-3}$ (bold lines). Elevation is contoured every 250 m (light lines).

5.2. Validation of model results

In order to investigate the advantages and shortcomings of the two different types of model initialisation and validate their results, it is necessary to see how both the VI and UI HYPACT concentration fields compare with the observed daily variation of pollutants during this episode. Figure 8 presents the daily variation of NO_x concentration measured by the air-quality monitoring station located in the centre of Athens (represented by a black rectangle in Figure 1) and the daily variation of the computed concentrations at the model grid point closest to the centre of Athens for both runs.

Comparison of the UI predicted concentrations with the observed ones shows that the model reproduces the observed morning maximum but a significant discrepancy is evident during the first hours of the simulation because the model does not take into account the pollutants trapped during the previous days. The time evolution of the observed and calculated concentrations present the same trend, but the late afternoon maximum (at 1800 UTC) is not quantitatively reproduced.

Comparison of the VI predicted concentrations with the observations shows that the model fails to reproduce the morning maximum, but later in the day the calculated and observed concentrations present the same trend and show a good quantitative agreement. The difference between the observed and VI run concentrations in the morning can be attributed to the fact that the dynamic and thermodynamic parameters in the ECMWF data are only given at three levels within the boundary layer (1000, 925 and 850 hPa) and with

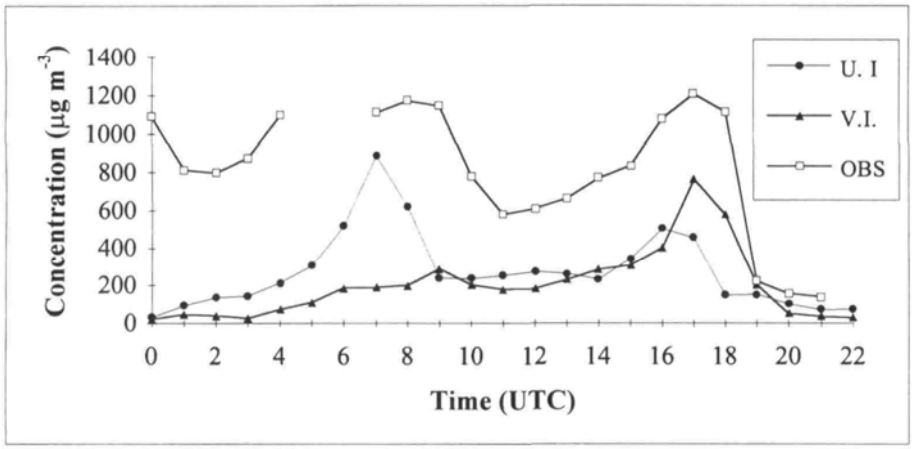

Figure 8. Time evolution of NO_x concentration from air-quality monitoring station in the centre of Athens (open rectangles) and of the computed concentration at the closest to the centre of Athens model grid point for the UI run (closed circles) and the VI run (closed triangles).

a horizontal resolution of 1 degree lat./lon.; therefore, the local boundary-layer characteristics are not well resolved. Later in the day the model is able to build up the local-scale circulations and this is the reason for the good agreement during the afternoon. On the other hand, the UI run which is initialised with the 0000 UTC, 18 January sounding predicts concentration fields in good agreement with the observations because the sounding profile is representative of the local-scale characteristics of the boundary layer with the strong surface inversion in the morning. Further, a reason for the quantitative discrepancy between observations and both runs is that the emission inventories assimilated in the model are mean annual values and therefore they are not representative of the emissions characterising the specific day of simulation.

6. Concluding remarks

In this study the RAMS-HYPACT modelling system has been applied in order to identify the capability of this modelling system to describe the transport and dispersion conditions characterising a severe air-pollution episode in an urban area. The complexity of the physiographic characteristics of the GAA under certain synoptic conditions, such as the presence of a high pressure system associated with weak pressure gradients, induce the development of local circulations which affect dramatically the dispersion conditions in the area. Therefore, in order to study air-pollution episodes in the region, use of a prognostic three-dimensional model, such as the RAMS-HYPACT modelling system, is necessary. This system simulates the time dependent three-dimensional fields of meteorological quantities and air-pollutant concentrations, taking into the account the physiographic variations in the area of interest as well as the rapidly changing synoptic, regional and local conditions. This approach is considered to be far superior to simpler techniques such as diagnostic meteorological models and Gaussian diffusion techniques, which may produce large errors in the advection and diffusion of the plume for many meteorological situations.

The application of the RAMS-HYPACT modelling system for a severe air-pollution episode case in GAA produced very promising results. The simulated meteorological fields reproduced well the conditions leading to high concentrations at the surface. The initialisation of RAMS with two different data-sets (one single sounding profile and ECMWF gridded data) identified the crucial role of model initialisation on air-quality simulations and the necessity of good vertical resolution of input data, especially within the boundary layer. More specifically, the uniform initialisation run provided reliable results during the morning hours, due to the representation of the surface inversion. The shortcoming of the uniform initialisation run is that the interaction of the synoptic and regional-scale forcing with the local scale cannot be reproduced. The variable initialisation run failed to reproduce the morning high concentrations due to the poor vertical resolution of input data. However, when the model started to build up the flow characteristics resulting from the interaction of the synoptic and regional-scale forcing with the local scale, the results were close to the observed values. Finally, a more accurate description of the emission inventories which would describe better the specific seasonal and daily emission characteristics would be necessary in order to reduce uncertainties.

Acknowledgements

The authors greatly acknowledge Prof. N. Moussiopoulos and Prof. I. Ziomas (University of Thessaloniki) for providing the emission inventories files used in this study. Dr C. Tremback of ASTER Division of Mission Research Corporation is kindly acknowledged for his help and comments on the models settings. Special thanks are also due to the editor R. W. Riddaway for his suggestions, which lead

to an improvement in the organisation, English and grammar of the text. Acknowledgement is made to the National Center for Atmospheric Research, which is sponsored by the National Science Foundation, for the computing time used in this research (Contract #35081147), and for providing the sounding and surface data used in this study. Special thanks are also due to the Program for Air Quality Monitoring in Athens (PERPA) and especially Mr A. Fotopoulos for providing the air-quality data for the selected case.

References

Fast, J. D., O'Steen, B. L. & Addis, R. P. (1995). Advanced atmospheric modelling for emergency response. *J. Appl. Meteorol.*, **34:** 626–649.

Kallos, G. & Kassomenos, P. (1994). Effects of the selected domain in mesoscale atmospheric simulations and dispersion calculations. In *Proc. of the 20th ITM of NATO/CCMS on Air Pollution Modeling and its Application*, ed. S. Gryning & M. Millan, vol. X, 35–44. Plenum Press.

Kallos, G., Kassomenos, P. & Pielke, R. A. (1993). Synoptic and mesoscale weather conditions during air pollution episodes in Athens, Greece. *Boundary-Layer Meteorol.*, **62:** 163–184.

Kassomenos, P., Kotroni, V. & Kallos, G. (1995). Analysis of the climatological and air quality observations from the Greater Athens Area. *Atmos. Environ.*, **29:** 3671–3688.

Lyons, W. A., Pielke, R. A., Cotton, W. R., Uliasz, M., Tremback, C. J., Walko, R. L. & Eastman, J. L. (1993). The applications of new technologies to modelling mesoscale dispersion in coastal zones and complex terrain. *In Air Pollution*, ed. P. Zannetti *et al.*, 35–85. Elsevier.

Lyons, W. A., Pielke, R. A., Cotton, W. R., Tremback, C. J., Walko, R. L., Uliasz, M. & Ibarra, J. I. (1994). Recent applications of the RAMS meteorological and the HYPACT dispersion models. *In Proc. of the 20th ITM of NATO/CCMS on Air Pollution Modeling and its Application*, ed. S. Gryning & M. Millan. Vol. X, 19–26. Plenum Press.

Lyons, W. A., Tremback, C. J., & Pielke, R. A., (1995). Applications of the Regional Atmospheric Modeling System (RAMS) to provide input to photochemical grid models for the Lake Michigan Ozone Study (LMOS). *J. Appl. Meteorol.*, **34:** 1762–1786.

Pielke, R. A., McNider, R. T., Segal, M. & Mahrer, Y. (1983). The use of a mesoscale numerical model for evaluations of pollutant transport and diffusion in coastal regions and over irregular terrain. *Bull. Am. Meteorol. Soc.*, **64:** 243–249.

Pielke, R. A., Lyons, W. A., McNider, R. T., Moran, M. D., Stocker, R. A., Walko, R. L. & Uliasz, M. (1991). Regional and mesoscale meteorological modelling as applied to air-quality studies. *In Air Pollution Modelling and its Applications VIII*, ed. H. van Dop and D.G. Steyn, 259–290. Plenum Press.

Pielke, R. A., Cotton, W. R., Walko, R. L., Tremback, C. J., Lyons, W. A., Grasso, L. D., Nicholls, M. E., Moran, M. D., Wesley, D. A., Lee, T. J. & Copeland, J. H. (1992). A comprehensive meteorological modelling system – RAMS. *Meteorol. Atmos. Phys.*, **49:** 69–91.

Poulos, G. S. & Bossert, J. E. (1995). An observational and prognostic numerical investigation of complex terrain dispersion. *J. Appl. Meteorol.*, **34:** 650–669.

Tremback, C. J., Lyons, W. A., Thorson, W. P. & Walko, R. L. (1994). An emergency response and local weather forecasting software system. In *Proc. of the 20th ITM of NATO/CCMS on Air Pollution Modeling and its Application*, ed. S. Gryning & M. Millan, vol. X: 423–429. Plenum Press.

Walko, R. L. & Tremback, C. J. (1991). *RAMS–The Regional Atmospheric Modelling System: User's Guide*. ASTeR Inc. P.O. Box 466, Fort Collins. Colorado, 86 pp.